

Cite this: DOI: 10.1039/c2cc36263e

www.rsc.org/chemcomm

COMMUNICATION

Multifunctional organic fluorescent materials derived from 9,10-distyrylanthracene with alkoxy endgroups of various lengths†

Xiqi Zhang,^a Zhenguo Chi,^{*a} Bingjia Xu,^a Long Jiang,^a Xie Zhou,^b Yi Zhang,^a Siwei Liu^a and Jiarui Xu^a

Received 28th August 2012, Accepted 17th September 2012

DOI: 10.1039/c2cc36263e

A series of remarkable multifunctional 9,10-distyrylanthracene derivatives (DSA_n , $n = 7-12$) was synthesized. All derivatives possess typical aggregation-induced emission (AIE) property. Some of the derivatives exhibit multifunctional properties, including AIE, mechanofluorochromism, vapochromism, thermochromism, and mesomorphism, which are rarely found to exist simultaneously in a single compound.

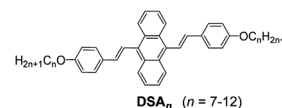
Most organic luminescent materials exhibit very strong luminescence in their dilute solutions. However, their light emissions dramatically decrease because of increased solution concentration or aggregation in the solid states, resulting from strong intermolecular π - π stacking interactions and nonradiative decay. This phenomenon is well known as the aggregation-caused quenching (ACQ).¹ The ACQ effect has greatly limited the applications of organic luminescent materials and has driven researchers to seek anti-ACQ materials with higher efficiency in the aggregated state than in the dissolved state. Some anti-ACQ materials have been reported by Tang *et al.*² and Park *et al.*³ in 2001 and 2002, respectively, and were called aggregation-induced emission (AIE) or aggregation-induced emission enhancement (AIEE) materials. Since then, AIE or AIEE materials have been found promising as emitters for the fabrication of highly efficient electroluminescent devices and as stimuli-responsive materials of probes.⁴ Since 2010, many AIE materials were reported to possess mechanofluorochromic properties.⁵ Herein, a series of compounds, DSA_n ($n = 7$ to 12; Scheme 1), was synthesized and found to exhibit at least five functions: AIE, mechanofluorochromism, vapochromism, thermochromism, and mesomorphism.

AIE phenomenon: as shown in Fig. 1a, DSA_{11} in pure THF exhibited a very weak photoluminescence (PL) intensity.

^a PCFMLab, DSAPM Lab, KLGHEI of Environment and Energy Chemistry, State Key Laboratory of Optoelectronic Materials and Technologies, School of Chemistry and Chemical Engineering, Sun Yat-sen University, Guangzhou 510275, P. R. China.
E-mail: chizhg@mail.sysu.edu.cn; Fax: +86 20 84112222;
Tel: +86 20 84112712

^b School of Pharmaceutical Sciences, Sun Yat-sen University, Guangzhou 510275, P. R. China

† Electronic supplementary information (ESI) available: Experimental details; Tables S1 and S2; Fig. S1–S14; Video S1, ¹H NMR, ¹³C NMR and MS spectra (Fig. S15–S32); crystallographic data (Tables S3–S8) (PDF). CCDC 886641–886646. For ESI and crystallographic data in CIF or other electronic format see DOI: 10.1039/c2cc36263e

Scheme 1 Chemical structure of DSA_n .

However, the PL intensity was significantly enhanced when the water fraction exceeded 40%. The PL intensity in pure THF was 5.4 a.u., which increased to ~ 295.8 a.u. in the 60% water–THF mixture, showing an approximately 55-fold enhancement. The ultraviolet–visible absorption spectra (UV-vis) of DSA_{11} in the water–THF mixtures are shown in Fig. 1b. The spectral profile was virtually unchanged even when a water fraction of up to 40% was added to the THF solution. With the further increased water fraction, the entire spectrum started to rise. The increase of the absorbance in the entire spectral region was caused by the Mie effect⁶ of the nano-aggregate suspensions in the solvent mixtures. The result showed that the DSA_{11} molecules started to aggregate markedly when the mixture contained 40% of water. The PL and UV-vis results were in good agreement. These results confirmed that the compound had a significant AIE effect caused by the formation of molecular aggregates upon the addition of water to the solution. Similar phenomena were observed for the other compounds (Fig. S1 and S2, ESI†).

The PL intensities of all the compounds decreased in the THF–water mixtures containing 50% and/or 60% of water.

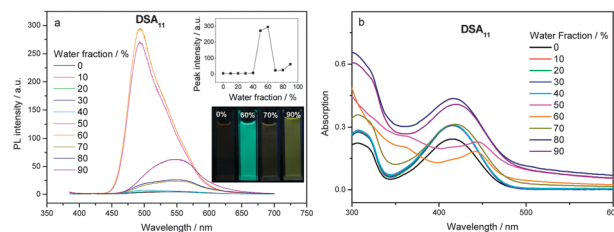


Fig. 1 (a) PL spectra of the dilute solutions of DSA_{11} (10 μ M) in water–THF mixtures with different volume fractions of water (excitation wavelength = 365 nm). The top inset shows the changes in the PL peak intensity. The bottom inset shows the emission images of DSA_{11} (10 μ M) in pure THF as well as 60%, 70%, and 90% water fraction mixtures under 365 nm UV illumination; (b) UV-vis absorption spectra of the dilute solutions of DSA_{11} (10 μ M) in water–THF mixtures with different volume fractions of water.

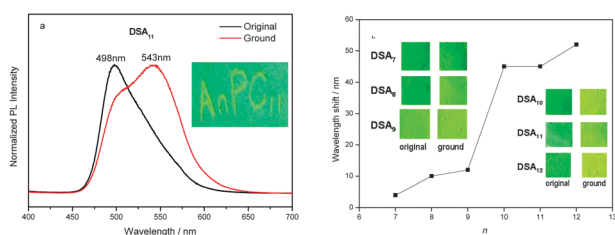


Fig. 2 (a) Normalized PL spectra of **DSA₁₁** before and after grinding, and (b) wavelength change *versus* *n* after grinding. Inset images: **DSA₁₁** cast on a filter paper, with “AnPC₁₁” written using a metal spatula at room temperature under UV light; images of the compounds before and after grinding under 365 nm UV illumination.

This phenomenon is often observed in some compounds with AIE properties, but the reasons remain unclear.⁷

Mechanofluorochromism: **DSA₁₀**, **DSA₁₁**, and **DSA₁₂** showed significant changes in emission when they were ground, *i.e.*, red shifting by 45, 45, and 52 nm, respectively (Table S1 and Fig. S3, ESI[†]). For example, the as-synthesized **DSA₁₁** showed a strong green emission (498 nm) under 365 nm UV light. After grinding, the sample showed a strong yellow emission (543 nm) with a 45 nm red-shift (Fig. 2a). These results indicated that **DSA₁₀**, **DSA₁₁**, and **DSA₁₂** have a color-switchable feature that has potential use in optical recording and pressure-sensing materials. However, **DSA₇**, **DSA₈**, and **DSA₉** exhibited insignificant mechanofluorochromism. After grinding, their emissions red shifted by only 4, 10, and 12 nm, respectively (Fig. 2b).

The X-ray structural analysis of the single crystals revealed that the compounds crystallized in the triclinic space group $P\bar{1}$. The selected dihedral angles between two phenyl rings and the anthryl ring, θ_{A-B} and θ_{B-C} (defined in Fig. S4, ESI[†]), are listed in Table S2 (ESI[†]). Analysis of the crystal structures of the compounds demonstrated that they have a nonplanar conformation in their crystals. The dihedral angle values in the molecular structures of the compounds optimized at the DFT B3LYP/6-31G level⁸ were the same, *i.e.*, θ_{A-B} and θ_{B-C} are equal to 60°. However, in their single crystals, the dihedral angles significantly differed. The conformation structures of **DSA₁₀**, **DSA₁₁**, and **DSA₁₂** were symmetrical; thus, the θ_{A-B} values were equal to θ_{B-C} and the values were 76°, 70°, and 74°, respectively. These values are greater than 60°, considering that the larger dihedral angles of the molecules were responsible for the shorter PL wavelengths (from 498 nm to 500 nm) in their original states. However, **DSA₇** and **DSA₈** crystals had two distinct conformation structures, namely, symmetric and asymmetric. In **DSA₇** crystals, θ_{A-B} and θ_{B-C} were 58° in the symmetric conformation structure, and 28° and 66° in the asymmetric conformation structure. In **DSA₈** crystals, θ_{A-B} and θ_{B-C} were 56° in the symmetric conformation structure, and 28° and 74° in the asymmetric conformation structure. **DSA₉** crystals had only an asymmetric conformation structure with $\theta_{A-B} = 40^\circ$ and $\theta_{B-C} = 50^\circ$. In general, the dihedral angles of **DSA₇**, **DSA₈**, and **DSA₉** were smaller than those of **DSA₁₀**, **DSA₁₁**, and **DSA₁₂**. Consequently, the former three compounds in their original states exhibited longer PL wavelengths (from 515 nm to 531 nm). The analysis of the crystal structures showed that the above mentioned difference among the molecular conformation structures of the crystals was caused by supramolecular

interactions including Ph → O, Ph → Ph, Ph → An, Oct → Ph, An → An, An → Ph, and Vin → An. Among these supramolecular interactions, CH- π interactions were the most important. The backbone of the molecules largely deviated from a plane, and typical cofacial π - π stacking became impossible because of the highly twisted conformation as well as steric hindrance of the bulky aromatic rings in the molecules. Thus, only **DSA₈** and **DSA₉** crystals exhibited weak face-to-face π -stacking of anthracene rings with small π -overlap areas and contact distances of about 3.64 Å (**DSA₈**) and 3.56 Å (**DSA₉**). As listed in Table S2 (also see Fig. S5, ESI[†]), **DSA₇**, **DSA₈**, and **DSA₉** crystals showed four, five, and four interactions; whereas **DSA₁₀**, **DSA₁₁**, and **DSA₁₂** crystals showed only one, two, and two supramolecular interactions, respectively. This result indicated that the supramolecular interactions in the former three crystals were stronger than those in the latter three crystals. The strong supramolecular interactions not only made the molecule more planar and stable in the lattice, but also induced tight intermolecular packing (Fig. S6, ESI[†]). The density *d* of **DSA₇**, **DSA₈**, and **DSA₉** crystals ranged from 1.167 g cm⁻³ to 1.185 g cm⁻³; for **DSA₁₀**, **DSA₁₁**, and **DSA₁₂** crystals, *d* ranged from 1.127 g cm⁻³ to 1.146 g cm⁻³, respectively. These results indicated that the more twisted conformation and weaker supramolecular interactions in **DSA₁₀**, **DSA₁₁**, and **DSA₁₂** crystals relatively loosened the molecular packing and resulted in lower lattice energies. The two structural features rendered the crystals easily destructible under external pressure. This is probably the reason why **DSA₁₀**, **DSA₁₁**, and **DSA₁₂** exhibited more significant mechanofluorochromism as compared to others.

Powder wide-angle X-ray diffraction measurements revealed the significantly different molecular packing structures of **DSA₁₀**, **DSA₁₁**, and **DSA₁₂** before and after grinding (Fig. S7, ESI[†]). The diffraction patterns of the as-synthesized samples displayed some sharp and intense reflections, which indicated some crystalline order. After grinding, the reflections remarkably weakened, indicating decrease in crystalline order. Notably, the three original samples had a strong reflection peak near $2\theta = 10^\circ$, which almost disappeared after grinding. However, **DSA₇**, **DSA₈**, and **DSA₉** had no such strong reflection peaks and their diffraction patterns changed little from their original forms after grinding. This finding further confirmed that the significant mechanofluorochromic properties of **DSA₁₀**, **DSA₁₁**, and **DSA₁₂** were caused by the change in crystalline order.

All the original compounds exhibited two marked exothermic transition peaks in heating differential scanning calorimetry (DSC) curves. One peak at the lower temperature was ascribed to the phase transition from solid crystalline to liquid crystal, T_{S-LC} , and the other peak at the higher temperature was ascribed to the phase transition from liquid crystal to isotropic melt, T_i . Grinding markedly affected the T_{S-LC} values of **DSA₁₀**, **DSA₁₁**, and **DSA₁₂**, including the position and shape of the transition peak, but hardly affected the T_i transition. For **DSA₇**, **DSA₈**, and **DSA₉**, almost no change in the two peaks was observed after grinding (Fig. S8, ESI[†]). The DSC results also indicated that grinding did significantly change the morphologies of **DSA₁₀**, **DSA₁₁**, and **DSA₁₂**.

The weighted mean lifetimes $\langle\tau\rangle$ are listed in Table S1 (ESI[†]). The $\langle\tau\rangle$ values of **DSA₇**, **DSA₈**, and **DSA₉** before

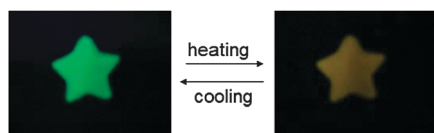


Fig. 3 Reversible color changes of DSA_{11} upon heating and cooling.

and after grinding were similar, and their time-resolved fluorescence curves almost coincided with one another (Fig. S9, ESI[†]). By contrast, the $\langle\tau\rangle$ values of the original and ground DSA_{10} , DSA_{11} , and DSA_{12} samples significantly differed: 1.22, 1.35, and 1.22 ns for the original samples; 3.42, 3.75, and 3.57 ns for the ground samples, respectively. These results showed that the time-resolved emission-decay behaviors of the original and ground compounds were distinctly changed when the materials showed significant mechanofluorochromic properties.

Thermochromism: all the compounds were found to possess thermochromic properties. As an example, a star-like pattern was stamped on a filter paper soaked in DSA_{11} solution in CH_2Cl_2 . After drying, the pattern emitted green light (514 nm) under 365 nm UV illumination. As the pattern was heated to the T_i transition of DSA_{11} using a hot air gun, its emission quickly changed to dark yellow (566 nm) and the variation in the emission wavelength reached 52 nm. As soon as the hot air gun was removed, the green emission pattern was immediately recovered, showing the excellent reversibility of the phenomenon (Fig. 3 and Video S1, ESI[†]). The temperature-dependent PL results of DSA_{11} are shown in Fig. S10 (ESI[†]).

Vapochromism: all the compounds exhibited vapochromism in their solid states. For example, under UV illumination (wavelength = 365 nm) at room temperature, a spot of DSA_{11} on the thin-layer chromatography (TLC) plate showed bright green fluorescence, which was reversibly switched off in an atmosphere of CH_2Cl_2 (Fig. S11, ESI[†]) or other viable solvent vapors. One probable explanation was that the solvation of the vapor of the appropriate solvent disrupted the interaction of solid molecules to a significant extent, resulting in the free rotation of the single bonds of the AIE molecules, which led to non-emission. The compounds possessed a reversible on–off fluorescence switching property in some organic vapors. Therefore, these compounds may be used as chemical vapor sensors in the photoswitch field, which may be one of their most important potential applications.

Mesomorphism: the DSC results showed that all the original samples had two endothermic peaks in the first heating process (Fig. S12, ESI[†]), indicating that two phases were present before isotropic melting. The peak at the higher temperature corresponding to T_i ranged from 166 °C to 129 °C. When $n < 10$, T_i decreased with increased n . When $n \geq 10$, T_i became independent of the chain length. However, the peak at the lower temperature (T_{S-LC}) strongly depended on the chain length and exhibited a zigzag pattern, showing a significant odd–even effect (Fig. S13, ESI[†]). This finding suggested that the direction of the chain-end can affect the molecular packing in the solid state and the thermal transition behavior. A colored birefringence-like thermotropic liquid crystalline texture appeared when the isotropic melt was cooled to below 130 °C (Fig. S14, ESI[†]).

In summary, a series of remarkable multifunctional 9,10-distyrylanthracene derivatives (DSA_n , $n = 7–12$) was successfully synthesized. All the derivatives are AIE compounds. When $n \geq 10$, the derivatives exhibit significant mechanofluorochromism. Supramolecular interaction was found to play an important role in determining the mechanofluorochromism. All the derivatives also exhibit vapochromism, thermochromism, and mesomorphism. These attributes may enable the application of these novel compounds in a wide range of fields, including optical displays, chemosensors, rewritable optical media, stress sensors, thermal sensors, among others.

The authors gratefully acknowledge the financial support from the National Natural Science Foundation of China (51173210, 51073177), the Science and Technology Planning Project of Guangdong Province, China (Grant numbers: 2007A010500001-2), Construction Project for University-Industry cooperation platform for Flat Panel Display from The Commission of Economy and Informatization of Guangdong Province (Grant number: 20081203), the Fundamental Research Funds for the Central Universities and Natural Science Foundation of Guangdong (S2011020001190).

Notes and references

- (a) R. H. Friend, R. W. Gymer, A. B. Holmes, J. H. Burroughes, R. N. Marks, C. Taliani, D. D. C. Bradley, D. A. Dos Santos, J. L. Bredas, M. Logdlund and W. R. Salaneck, *Nature*, 1999, **397**, 121; (b) S. A. Jenekhe and J. A. Osaheni, *Science*, 1994, **265**, 765; (c) C. T. Chen, *Chem. Mater.*, 2004, **16**, 4389.
- J. D. Luo, Z. L. Xie, J. W. Y. Lam, L. Cheng, H. Y. Chen, C. F. Qiu, H. S. Kwok, X. W. Zhan, Y. Q. Liu, D. B. Zhu and B. Z. Tang, *Chem. Commun.*, 2001, 1740.
- B. K. An, S. K. Kwon, S. D. Jung and S. Y. Park, *J. Am. Chem. Soc.*, 2002, **124**, 14410.
- (a) Y. N. Hong, J. W. Y. Lam and B. Z. Tang, *Chem. Commun.*, 2009, 4332; (b) Y. S. Zhao, H. B. Fu, A. D. Peng, Y. Ma, D. B. Xiao and J. N. Yao, *Adv. Mater.*, 2008, **20**, 2859; (c) B. J. Xu, Z. G. Chi, Z. Y. Yang, J. B. Chen, S. Z. Deng, H. Y. Li, X. F. Li, Y. Zhang, N. S. Xu and J. R. Xu, *J. Mater. Chem.*, 2010, **20**, 4135; (d) H. Y. Li, Z. G. Chi, B. J. Xu, X. Q. Zhang, Z. Y. Yang, X. F. Li, S. W. Liu, Y. Zhang and J. R. Xu, *J. Mater. Chem.*, 2010, **20**, 6103; (e) Z. Y. Yang, Z. G. Chi, B. J. Xu, H. Y. Li, X. Q. Zhang, X. F. Li, S. W. Liu, Y. Zhang and J. R. Xu, *J. Mater. Chem.*, 2010, **20**, 7352.
- (a) B. J. Xu, Z. G. Chi, X. Q. Zhang, H. Y. Li, C. J. Chen, S. W. Liu, Y. Zhang and J. R. Xu, *Chem. Commun.*, 2011, **47**, 11080; (b) H. Y. Li, X. Q. Zhang, Z. G. Chi, B. J. Xu, W. Zhou, S. W. Liu, Y. Zhang and J. R. Xu, *Org. Lett.*, 2011, **13**, 556; (c) X. Q. Zhang, Z. G. Chi, H. Y. Li, B. J. Xu, X. F. Li, W. Zhou, S. W. Liu, Y. Zhang and J. R. Xu, *Chem.–Asian J.*, 2011, **6**, 808; (d) X. Q. Zhang, Z. G. Chi, J. Y. Zhang, H. Y. Li, B. J. Xu, X. F. Li, S. W. Liu, Y. Zhang and J. R. Xu, *J. Phys. Chem. B*, 2011, **115**, 7606; (e) S. J. Yoon, J. W. Chung, J. Gierschner, K. S. Kim, M. G. Choi, D. Kim and S. Y. Park, *J. Am. Chem. Soc.*, 2010, **132**, 13675; (f) X. L. Luo, J. N. Li, C. H. Li, L. P. Heng, Y. Q. Dong, Z. P. Liu, Z. S. Bo and B. Z. Tang, *Adv. Mater.*, 2011, **23**, 3261; (g) C. D. Dou, L. Han, S. S. Zhao, H. Y. Zhang and Y. Wang, *J. Phys. Chem. Lett.*, 2011, **2**, 666; (h) X. Q. Zhang, Z. G. Chi, B. J. Xu, C. J. Chen, X. Zhou, Y. Zhang, S. W. Liu and J. R. Xu, *J. Mater. Chem.*, 2012, **22**, 18505.
- H. Tong, Y. Q. Dong, M. Häußler, J. W. Y. Lam, H. H. Y. Sung, I. D. Williams, J. Z. Sun and B. Z. Tang, *Chem. Commun.*, 2006, 1133.
- (a) S. C. Dong, Z. Li and J. G. Qin, *J. Phys. Chem. B*, 2009, **113**, 434; (b) Z. Y. Yang, Z. G. Chi, T. Yu, X. Q. Zhang, M. N. Chen, B. J. Xu, S. W. Liu, Y. Zhang and J. R. Xu, *J. Mater. Chem.*, 2009, **19**, 5541; (c) X. Q. Zhang, Z. G. Chi, B. J. Xu, H. Y. Li, Z. Y. Yang, X. F. Li, S. W. Liu, Y. Zhang and J. R. Xu, *Dyes Pigm.*, 2011, **89**, 56.
- M. J. Frisch, G. W. Trucks and H. B. Schlegel, *et al.*, *Gaussian 03, Revision D.01*, Gaussian, Inc., Wallingford, CT, 2004.